

Perturbed and Permuted

Signal Integration in Network-Structured Dynamic Systems

Dennis Wylie

November 4, 2018

Abstract

Biological systems (among others) may respond to a large variety of distinct external stimuli, or signals. These perturbations will generally be presented to the system not singly, but in various combinations, so that a proper understanding of the system response requires assessment of the degree to which the effects of one signal modulate the effects of another. This paper develops a pair of structural metrics for sparse differential equation models of complex dynamic systems and demonstrates that said metrics correlate with proxies of the susceptibility of one signal-response to be altered in the context of a second signal. One of these metrics may be interpreted as a normalized arc density in the neighborhood of certain influential nodes; this metric appears to correlate with increased independence of signal response.

1 Introduction

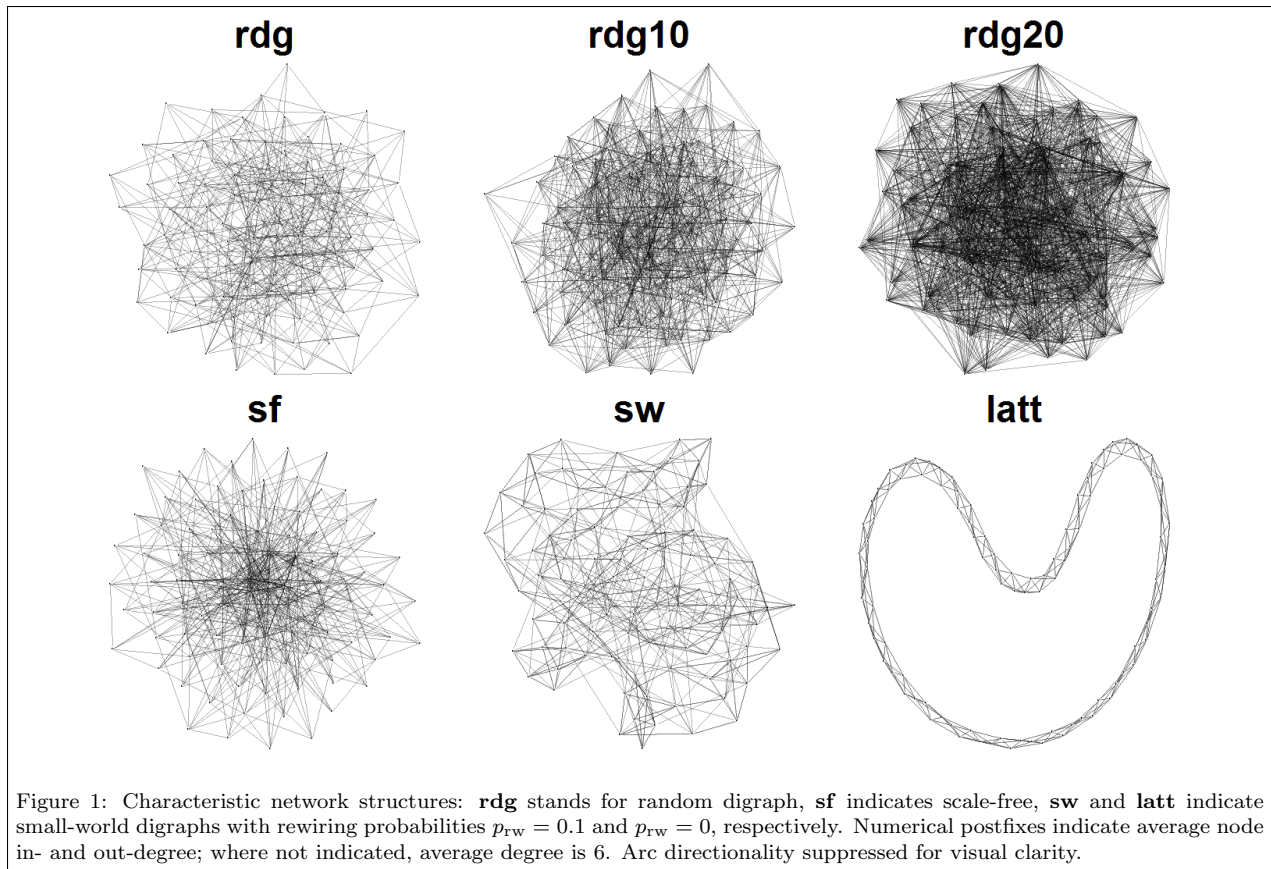
Biological signaling pathways frequently intersect one another, leading to the phenomenon of cross-talk, wherein the effect of one signaling pathway influences the activity of another. For example, during *Drosophila* development, the epidermal growth factor receptor (EGFR) and Notch signaling pathways interact both within and between cells, producing highly context-specific responses to their respective signals during the formation of spatially structured organs including the eye [1]. The interactions between these pathways range from antagonistic to cooperative across different processes and at different times within a given process, resulting in an intricate integration of signal response.

The concept of signal interaction embodied in this example can be generalized to less obvious biological examples as well: for instance, it has been suggested that cell-to-cell variation between embryonic stem (ES) cells may result in differential responses to

differentiation signals, thereby permitting some ES cells to undergo lineage specification while others remain pluripotent [2]. Regarding the differences in molecular population and configuration constituting such ES cellular variation as random perturbations (or more abstractly, signals) to the biochemical state, this phenomenon may also be described as the modulation by one signal of the systemic response to another.

A key question in such cases is to what extent the presence and magnitude of one signal interferes with or reinforces the effects of the other. Perhaps the simplest possibility is linear superposition, in which the system essentially responds with the sum of the responses it would have to the two signals if presented separately — i.e., despite making use of common signaling components, the two signals act in a fundamentally independent manner. Such “signal independence” is, however, inconsistent with many properties ascribed to the interlinked networks of biological signaling pathways. For instance, while an AND gate of sorts could be constructed with linear superposition of two signals if the effect of either one alone was below threshold, in the presence of noisy signals of widely varying magnitudes (more the rule than the exception in biological signaling), a particularly high magnitude single signal would lead to activation by itself. Meanwhile, even the complexity of a simple XOR (exclusive-or) gate would be impossible with linear signal superposition/signal independence.

Previous work by Wylie [3] suggests that the network topology of dynamic systems plays a key role in determining the integration of multistable dynamic “switches:” specifically, sparse networks of relatively homogenous node degree were found to be more favorable to switch integration than were dense or scale-free networks. Here we investigate whether similar ideas might be applied to wider class of signal integration phenomena not necessarily involving multistability.



2 Terminology and Notation

We consider deterministic nonlinear dynamic systems with steady state at the origin, so that

$$\begin{aligned} \frac{dx_i}{dt} &= f_i(\mathbf{x}) \\ &= \sum_j A_{ij}x_j + \sum_{j,k} B_{ijk}x_jx_k + O(x^3) \end{aligned} \quad (1)$$

For the purposes of this paper, we will restrict ourselves to quadratic systems for which all third-order and higher terms vanish, so that the linearization matrix A and the three-index array B (which, without loss of generality, we assume is symmetric with respect to its 2nd and 3rd indices) totally determine the dynamics. We will also write equation (1) as

$$\frac{d\mathbf{x}}{dt} = \mathbf{A}\mathbf{x} + \mathbf{B}(\mathbf{x}, \mathbf{x}) \quad (2)$$

Models of large biological systems are generally sparse in the sense that most entries A_{ij} in the matrix A vanish. We can thus associate a network structure

(more precisely, a directed graph in which “one-loop” arcs from a node i to itself are allowed) $G = (V_G, E_G)$ with the system by

$$(i \rightarrow j) \in E_G \text{ iff } A_{ji} \neq 0 \text{ (Note index order)} \quad (3)$$

We will assume here that the quadratic array B is consistent with the network structure G , in the sense that

$$B_{ijk} = 0 \text{ unless } (j \rightarrow i), (k \rightarrow i) \in E_G \quad (4)$$

which is necessary if the linearized system structure G is to be stable to small perturbations of the form

$$\mathbf{f}(\mathbf{x}) \mapsto \mathbf{f}(\mathbf{x}) + \Delta\mathbf{c} \quad (5)$$

as is discussed further in section 4. The network structures G considered in this work are generally random digraphs, scale-free digraphs characterized by high variance of node (in- and out-) degree, and small-world digraphs (including lattice digraphs) characterized by high clustering. (Here in-/out-degree are defined ignoring both one-loop arcs and arc weights.) Figure 1 offers visualizations of some characteristic structures.

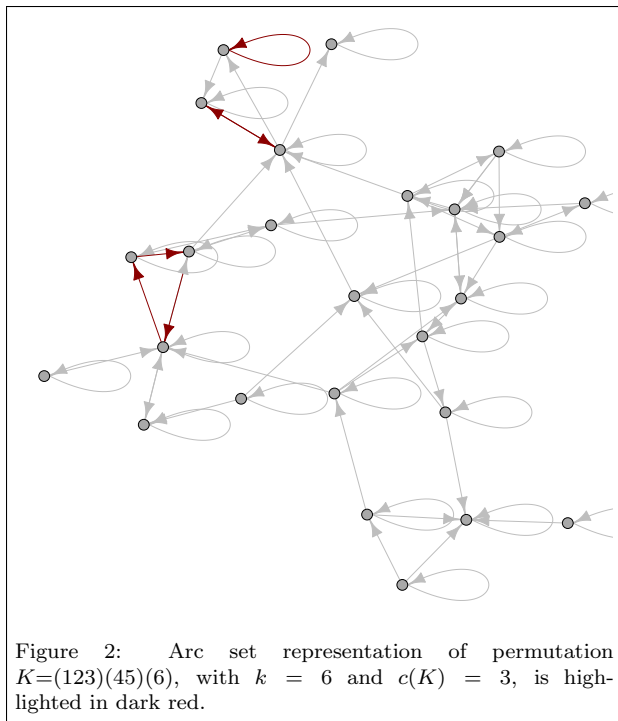


Figure 2: Arc set representation of permutation $K=(123)(45)(6)$, with $k = 6$ and $c(K) = 3$, is highlighted in dark red.

3 Topological Properties of Characteristic Polynomial

We here refer to the characteristic polynomial associated with the linearization matrix A ,

$$\det(A - \lambda I) = (-1)^{n-1} \sum_{k=0}^n F_{n-k} \lambda^k \quad (6)$$

as the characteristic polynomial of the system described by equation (1). The notation F_k used in equation (6) is intended to evoke the interpretation of the coefficients of the characteristic polynomial as the “feedback at length k ” in the (weighted) network G . This interpretation stems from the relationship [4, 5]

$$F_k = \sum_{K \in \Theta_k} \left[(-1)^{c(K)+1} \prod_{(i \rightarrow j) \in K} A_{ji} \right] = \sum_{K \in \Theta_k} w_K \quad (7)$$

where Θ_k is the set of all permutations of k integers chosen from the set $\{1, 2, \dots, n\}$. Here we regard any particular permutation K chosen from Θ_k as a set of arcs $(i \rightarrow j)$ corresponding to the mappings of individual elements by the permutation operation (illustrated in figure 2). Considering the standard cycle representation of permutation groups [6], it is

apparent that, considered graphically, K will generally consist of a definite number $c(K)$ of node-disjoint cycles, the sum of whose lengths is k . We define here the weight w_K of the permutation K with respect to the system A to be the product of the arc weights A_{ji} associated with the arcs $(i \rightarrow j)$ making up K (times the sign factor $(-1)^{c(K)+1}$), so that F_k is simply the sum of the length- k permutation cycle weights. This is the basis for considering F_k as a measure of feedback (of length k) in the linearized system A .

4 Variation under System Perturbation

We take signal inputs to our dynamic systems in the form of perturbations to the system dynamics

$$\mathbf{f}(\mathbf{x}) \mapsto \mathbf{f}(\mathbf{x}) + \Delta \mathbf{c} \quad (8)$$

In the context of a biochemical model, signals described by equation (8) might consist of the steady input and/or removal of a given set of chemical species.

For small perturbations, the root $\Delta \mathbf{y}$ ($= \Delta \mathbf{y}^{(1)} + \Delta \mathbf{y}^{(2)} +$ higher order terms) of the function $(\mathbf{f} + \Delta \mathbf{c})$ is given to first order in $\Delta \mathbf{c}$ by

$$\Delta \mathbf{y}^{(1)} = -A^{-1} \Delta \mathbf{c} \quad (9)$$

If the system is perturbed by two distinct perturbations $\Delta \mathbf{c}$ and $\delta \mathbf{c}$ — representing here two incoming signals — the first order root shift response ($\Delta \mathbf{y}^{(1)} + \delta \mathbf{y}^{(1)}$) will obviously be a linear superposition of the responses to the two individual signals input singly. We then consider also the second order mixed terms,

$$\Delta \delta \mathbf{y}^{(2)} = -2A^{-1} B(\Delta \mathbf{y}^{(1)}, \delta \mathbf{y}^{(1)}) \quad (10)$$

As the only terms we will be interested in of greater than first order will be mixed terms of the $\Delta \delta$ form, we will henceforth drop the parenthetical superscripts.

We here consider two distinct outputs, in the form of changes to the steady-state properties of the dynamic system under consideration, resulting from the signal inputs $\Delta \mathbf{c}$ and $\delta \mathbf{c}$. These are the coefficients of the characteristic polynomial F_k (for brevity, we will generally refer simply to “the characteristic polynomial F_k ”) and the eigenvalues λ (particularly the “least stable” eigenvalue(s) λ_{ls} of largest real part $\text{Re}(\lambda)$). These particular outputs were chosen for their close relationship with system stability, as well as for some degree of analytic convenience.

One simple metric for quantifying the degree to which a signal $\Delta \mathbf{c}$ applied to the system \mathbf{f} may be expected to change the effects of a randomly distributed second signal $\delta \mathbf{c}$ with regard to a particular output function U is the Pearson correlation

$$\begin{aligned} \text{Corr}_\delta(\delta U + \Delta \delta U, \delta U) & \quad (11) \\ &= 1 + \frac{\langle\langle \delta U \Delta \delta U \rangle\rangle_\delta^2}{2 \langle\langle [\delta U]^2 \rangle\rangle_\delta^2} - \frac{\langle\langle [\Delta \delta U]^2 \rangle\rangle_\delta}{2 \langle\langle [\delta U]^2 \rangle\rangle_\delta} + \text{H.O.T.} \end{aligned}$$

where the correlation and (co)variances are all taken with respect to the distribution of $\delta \mathbf{c}$ (the notation $\langle\langle XY \rangle\rangle$ indicates the covariance of the random variables X and Y). Equation (11) is a simple lowest order expansion of the Pearson correlation in $\Delta \delta U$. It is worth noting that since we are considering a quantity which clearly depends on the overall scale of the perturbations δU , ΔU , and $\Delta \delta U$, and since we would like to compare this quantity across systems with very different structures, we must consider how to properly normalize the signals $\delta \mathbf{c}$ and $\Delta \mathbf{c}$. For the purposes of this work, signals were normalized by the root-mean-square average magnitudes of the first-order shifts $\delta \lambda_{\text{is}}$ to the least-stable (largest real-part) eigenvalues of the linearization matrix A (see sections 6 - 7).

To apply equation (11) to our cases of interest ($U = F_k$ or $U = \lambda_{\text{is}}$), we must thus obtain estimates of δF_k , $\Delta \delta F_k$, $\delta \lambda_{\text{is}}$, and $\Delta \delta \lambda_{\text{is}}$. These estimates are primarily obtained through numerical methods, but it is of interest to derive formulae for a few of them in terms of the system parameters A and B . Linearizing around the shifted steady state $\delta \mathbf{y}$, we find that the linearization matrix A is shifted to $A + \delta A$, with δA given by

$$\delta A_{ij} = 2 \sum_k B_{ijk} \delta y_k \quad (12)$$

and

$$\Delta \delta A_{ij} = 2 \sum_k B_{ijk} \Delta \delta y_k \quad (13)$$

Equation (12) also provides the rationale for the consistency constraints on the entries of array B mentioned in section 2 above, since for any arc $(j \rightarrow i) \notin E_G$, $\delta A_{ij} = 0$ for all perturbations $\delta \mathbf{y}$ requires $B_{ijk} = B_{ikj} = 0$ for all k .

The shift in the system steady state to $\delta \mathbf{y}$ under the perturbation $\delta \mathbf{c}$ then induces a shift in the characteristic polynomial given by

$$\delta F_k = \sum_{i,j} \frac{\partial F_k}{\partial A_{ij}} \delta A_{ij} \quad (14)$$

while under the combination of perturbations $\delta \mathbf{y}$ and $\Delta \mathbf{y}$,

$$\Delta \delta F_k = \sum_{i,j} \left[\frac{\partial F_k}{\partial A_{ij}} \Delta \delta A_{ij} + \sum_{(q,r) \neq (i,j)} \frac{\partial^2 F_k}{\partial A_{ij} \partial A_{qr}} \Delta A_{ij} \delta A_{qr} \right] \quad (15)$$

where the range of the second summation in equation (15) excludes the pair (i, j) because F_k , as defined by equation (7) above, is a polynomial in the entries of the matrix A in which all terms are of order 0 or 1 in any given matrix entry A_{ij} (that is, F_k is a ‘‘multi-affine’’ function of the entries of A).

Finally, we are interested also in the shift $\delta \lambda$ in the eigenvalues λ under the perturbation $\delta \mathbf{c}$. Noting that the eigenvalues λ must be roots of the characteristic polynomial,

$$\sum_k (F_{n-k} + \delta F_{n-k})(\lambda + \delta \lambda)^k = 0 \quad (16)$$

may be used to derive

$$\delta \lambda = \frac{-\sum_k \delta F_{n-k} \lambda^k}{\sum_k k F_{n-k} \lambda^{k-1}} \quad (17)$$

A similar equation could be derived from equation (16) for the mixed term $\Delta \delta \lambda$, but in the interest of brevity, we will not consider it explicitly. Instead, we will note only that the functional dependence of the eigenvalues λ on the characteristic polynomial implies that the variation $\Delta \delta \lambda$ must be a function of the variations δF_k , ΔF_k , and $\Delta \delta F_k$ (as well as the unperturbed eigenvalue λ).

5 Sparse Matrices

Consider a distribution of systems for which the structure G is a random digraph in which each arc is included with independent probability p_{arc} , and for which all included arcs $(j \rightarrow i) \in E_G$ have linearization weight A_{ij} drawn from a given probability density function $p_{\text{wt}}(x)$ independently of the weights of all other entries (arcs). Then with probability $(1 - p_{\text{arc}}^k)$ the weight w_K of any particular k -permutation term (henceforward k -term) K in equation (7) is 0, while with probability p_{arc}^k , it is distributed according to the density function

$$\begin{aligned} p_{k\text{-wt}}(w_K \mid K \subset E_G) & \quad (18) \\ &= \int p_{\text{wt}} \left(\left[\prod_{i=1}^{k-1} \frac{1}{x_i} \right] w_K \right) \left[\prod_{i=1}^{k-1} \frac{p_{\text{wt}}(x_i)}{|x_i|} \right] d^{k-1}x \end{aligned}$$

since all k arcs making up K are independent and identically distributed. We further take p_{wt} symmetric about 0 (so that the mean of each matrix entry is 0). Thus, we consider the mean-square expectation value for w_K for any k -term K :

$$\begin{aligned} \langle w_K^2 \rangle &= p_{\text{arc}}^k \langle w_{(+,k)}^2 \rangle \\ &= p_{\text{arc}}^k \int w_K^2 p_{k\text{-wt}}(w_K | K \subset E_G) dw_K \end{aligned} \quad (19)$$

where $\langle w_{(+,k)}^2 \rangle$ is defined with respect to the distribution assuming all arcs in the k -term considered are present in the matrix A . Note particularly that $\langle w_{(+,k)}^2 \rangle$ does not depend on p_{arc} . Finally, we also note that any two k -terms K_1 and K_2 are distinct if and only if each of K_1 and K_2 contains at least one arc not contained in the other: but in this case they must have zero covariance $\langle w_{K_1} w_{K_2} \rangle = 0$, since the (zero-mean) weight of each arc is independent of that of all others. Noting also that $\langle w_K \rangle = 0$ for all $K \in \Theta_K$ — and hence $\langle F_k \rangle = 0$ — the mean-square value of the k^{th} coefficient of the characteristic polynomial is

$$\begin{aligned} \langle F_k^2 \rangle &= \sum_{K \in \Theta_k} \langle w_K^2 \rangle = \sum_{\Theta_k} p_{\text{arc}}^k \langle w_{(+,k)}^2 \rangle \\ &= \binom{n}{k} k! p_{\text{arc}}^k \langle w_{(+,k)}^2 \rangle \end{aligned} \quad (20)$$

Now consider adding an additional δA_{qr} to the matrix entry A_{qr} . This will result in a change δF_k proportional to the sum of the weights of all k -terms K containing the arc $(r \rightarrow q)$. As there are $N_{k;qr} = \binom{n-2+\delta_{rq}}{k-2+\delta_{rq}} (k-1)!$ possible k -terms passing through the arc $(r \rightarrow q)$, each having probability p_{arc}^{k-1} of being present (given the presence of the arc $(r \rightarrow q)$), the mean-square expectation value of δF_k is given by

$$\langle [\delta F_k]_{(r \rightarrow q)}^2 \rangle = N_{k;qr} p_{\text{arc}}^{k-1} \langle w_{(+,k-1)}^2 \rangle [\delta A_{qr}]^2 \quad (21)$$

(Note the covariance of δF_k with F_k vanishes owing to the symmetry of p_{wt} .) Now consider adding additional weight δA_{qr} and ΔA_{uv} to the two arcs $(r \rightarrow q)$ and $(v \rightarrow u)$. Similar considerations then lead to

$$\begin{aligned} \langle [\Delta \delta F_k]_{(v \rightarrow u), (r \rightarrow q)}^2 \rangle \\ = N_{k;qr uv} p_{\text{arc}}^{k-2} \langle w_{(+,k-2)}^2 \rangle [\Delta A_{uv} \delta A_{qr}]^2 \end{aligned} \quad (22)$$

where the final term corresponds to the $N_{k;qr uv} = (1-\delta_{rv})(1-\delta_{qu}) \binom{n-4+\delta_{qr}+\delta_{uv}+\delta_{qv}+\delta_{ru}}{k-4+\delta_{qr}+\delta_{uv}+\delta_{qv}+\delta_{ru}} (k-2)!$ possible k -terms passing through both $(r \rightarrow q)$ and $(v \rightarrow u)$.

From equations (19)-(22), we can thus deduce that

$$\frac{\partial \sqrt{\langle F_k^2 \rangle}}{\partial A_{qr}} \propto p_{\text{arc}}^{\frac{1}{2}(k-1)}, \quad \text{while} \quad \frac{\partial^2 \sqrt{\langle F_k^2 \rangle}}{\partial A_{qr} \partial A_{uv}} \propto p_{\text{arc}}^{\frac{1}{2}(k-2)} \quad (23)$$

from which we can conclude that for denser matrices (higher values of p_{arc}), the ratio of second- to first-derivatives of the root-mean-square expectation value of the coefficients of the characteristic polynomial F_k with respect to arc weights is generally lower than for sparser matrices.

Noting that under the variation $A \mapsto A + \delta A + \Delta A$,

$$\begin{aligned} \frac{\langle \langle [\Delta \delta F_k]^2 \rangle \rangle_{\delta}}{\langle \langle [\delta F_k]^2 \rangle \rangle_{\delta}} = \\ \frac{\sum_{i,j,q,r,s,u,v,w} \left[\frac{\partial^2 F_k}{\partial A_{ij} \partial A_{qr}} \frac{\partial^2 F_k}{\partial A_{su} \partial A_{vw}} * \right]}{\sum_{i,j,q,r} \frac{\partial F_k}{\partial A_{ij}} \frac{\partial F_k}{\partial A_{qr}} \langle \langle \delta A_{ij} \delta A_{qr} \rangle \rangle} \end{aligned} \quad (24)$$

we see that decreasing the relative sizes of the second derivatives of F_k compared to the first derivatives might be expected to result in decreased values of the negative term in equation (11) (with $U = F_k$) for the correlation $\text{Corr}_{\delta}(\delta F_k + \Delta \delta F_k, \delta F_k)$.

At this point it should be noted that the conditions under which equations (18)-(24) were derived are quite restrictive and unrealistic if taken to describe the linearization matrices A associated with systems \mathbf{f} modeling biological systems. The simple random digraphs taken as the network structures G (especially the treatment of diagonal one-loop arcs $(i \rightarrow i)$ symmetrically with all other arcs $(r \rightarrow q)$) and the assumption of independence of arc weights both neglect important features of real dynamic systems. In particular, under these assumptions it is almost certain that the matrix A will have some eigenvalues with positive real part, and hence will not describe the linearization of a system \mathbf{f} about a stable steady state.

We do not attempt to address these points analytically, but instead shift our attention to numerical investigation of specific systems with more complex (and realistic) features. This also allows us to consider another dynamic system property — the distance $\text{Re}(\lambda_{\text{is}})$ from the set of eigenvalues of A to the imaginary axis in the complex plane (here designated the eigenvalue stability) — which is of more immediate use in determining system stability.

6 Arc-Derivative Ratios for Stabilized Matrices

We first consider the impact of requiring system stability — i.e., all eigenvalues of the linearization matrix A must be in the left half of the complex plane — on the ratio of second derivatives of the determinant or the eigenvalue stability to the first derivatives with respect to the arc weights A_{ij} . Here we enforce this requirement on each matrix A by subtracting $(\text{Re}(\lambda_{\text{ls}})+1)I$ from A , where λ_{ls} is (one of) the largest real-part eigenvalue(s) of A , so that the new version of A will always have eigenvalue stability -1. (From the point of view of the network G corresponding to the matrix A , this operation consists of adding all one-loop arcs to G with weight $-(\text{Re}(\lambda_{\text{ls}}) + 1)$.)

In order to characterize the magnitudes of second- relative to first-derivatives of both the determinants $\det(A) = (-1)^{n-1}F_n$ and the eigenvalue stabilities $\text{Re}(\lambda_{\text{ls}})$ with respect to arc weights A_{ij} for a given matrix A with randomly constructed network structure G , we numerically evaluated the 25 first derivatives and 625 second derivatives of both metrics with respect to a set E_{ptb} containing 25 arcs randomly chosen from the arc set E_G . The root-mean-square (rms) average of the 625 second derivative terms was then divided by the rms average of the 25 first derivative terms to yield a single value

$$\frac{\sqrt{\frac{1}{|E_{\text{ptb}}|^2} \sum_{(j \rightarrow i), (r \rightarrow q) \in E_{\text{ptb}}} \left[\frac{\partial^2 U}{\partial A_{ij} \partial A_{qr}} \right]^2}}{\sqrt{\frac{1}{|E_{\text{ptb}}|} \sum_{(j \rightarrow i) \in E_{\text{ptb}}} \left[\frac{\partial U}{\partial A_{ij}} \right]^2}} \quad (25)$$

of this ratio for each matrix A for each of the two metrics (determinant and eigenvalue stability).

As mentioned in section 4 above, when comparing the response of systems with widely varying structures to parametric perturbation, a measure of the perturbation size is required. For our purposes, it is natural to use the induced change to the eigenvalue stability as an indicator of the relative magnitude of a given perturbation, especially given that we have already normalized all of our stabilized systems to have the same base eigenvalue stability value of -1. In the discussion to follow, we thus also present results for (rms averages of) derivatives with respect to the scaled arc weights

$$\tilde{A}_{ij} = \frac{1}{\epsilon} \sqrt{\left\langle [\Delta \text{Re}(\lambda_{\text{ls}})]^2 \right\rangle_{E_{\text{ptb}}}} A_{ij} \quad (26)$$

where

$$\left\langle [\Delta \text{Re}(\lambda_{\text{ls}})]^2 \right\rangle_{E_{\text{ptb}}} = \frac{\epsilon^2}{|E_{\text{ptb}}|} \sum_{(j \rightarrow i) \in E_{\text{ptb}}} \left[\frac{\partial \text{Re}(\lambda_{\text{ls}})}{\partial A_{ij}} \right]^2 \quad (27)$$

is approximately equal to the mean-square variation of $\text{Re}(\lambda_{\text{ls}})$ if the weights of the arcs in E_{ptb} are subjected to independent Gaussian perturbations of equal (small) variance $\frac{\epsilon^2}{|E_{\text{ptb}}|}$. The resulting scaled derivatives are then

$$\frac{\partial U}{\partial \tilde{A}_{ij}} = \frac{1}{\epsilon} \left\langle [\Delta \text{Re}(\lambda_{\text{ls}})]^2 \right\rangle_{E_{\text{ptb}}}^{-\frac{1}{2}} \frac{\partial U}{\partial A_{ij}} \quad (28)$$

and

$$\frac{\partial^2 U}{\partial \tilde{A}_{ij} \partial \tilde{A}_{qr}} = \frac{1}{\epsilon^2} \left\langle [\Delta \text{Re}(\lambda_{\text{ls}})]^2 \right\rangle_{E_{\text{ptb}}}^{-1} \frac{\partial^2 U}{\partial A_{ij} \partial A_{qr}} \quad (29)$$

where U is either the determinant $\pm F_n$ or the eigenvalue stability $\text{Re}(\lambda_{\text{ls}})$. This scaling is specifically indicated where it has been applied. Clearly, for $U = \text{Re}(\lambda_{\text{ls}})$, one result of such scaling will be to bring the rms average of the first derivatives to unity.

Figure 3 then shows the first, second (median), and third quartiles of these ratios calculated from populations of stabilized random digraphic-structured matrices with varying arc density (100 matrices, each with a different structure G and $n = 100$, were generated for each arc density grouping). Both the unscaled and scaled data exhibit the expected trend of decreasing rms magnitudes of second derivatives compared to first derivatives for metric U chosen to be either determinant or eigenvalue stability.

While these results suggest that the qualitative effects of network density suggested by equations (23) still hold for stabilized random digraphical systems with varying arc densities (and perturbation sensitivities), we have not yet considered more complex structural variation. We also have not yet considered correlation under variation of the offset parameters originally introduced in section 4, as opposed to the derivatives with respect to individual arc weights considered in this section. The behavior of these correlations (for random digraphical systems of varying arc density, for scale-free systems characterized by large node degree heterogeneity, and for highly clustered small-world systems) is investigated in the next section.

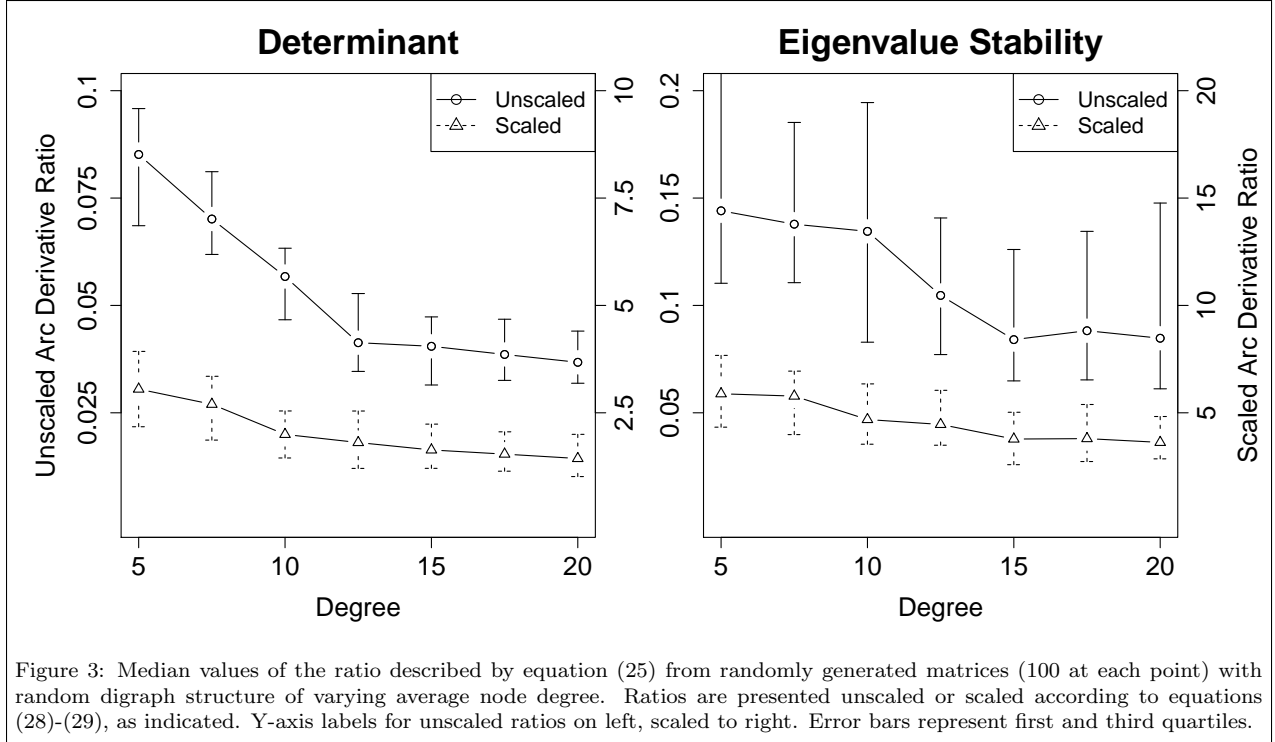


Figure 3: Median values of the ratio described by equation (25) from randomly generated matrices (100 at each point) with random digraph structure of varying average node degree. Ratios are presented unscaled or scaled according to equations (28)-(29), as indicated. Y-axis labels for unscaled ratios on left, scaled to right. Error bars represent first and third quartiles.

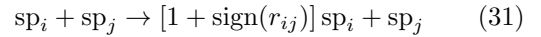
7 Correlation Susceptibility in Perturbed Dynamic Systems reaction

In order to study the effects of network structure on signal integration in non-linear dynamic systems described by equation (2), it is necessary to consider not only the network structure G and the linearization matrix A , but also the quadratic terms B . For the purposes of this paper, random systems were constructed by first generating a random network G (according to one of the random digraph generation algorithms described in appendix A), followed by progressively building up A and B as follows.

For each arc $(j \rightarrow i) \in E_G$, we generate a random “rate constant” r_{ij} from a Gaussian distribution of vanishing mean and unit variance independent of all other system parameters and reset

$$\begin{aligned} A_{ij} &\mapsto A_{ij} + r_{ij} \\ B_{iji} &\mapsto B_{iji} + \frac{1}{2}r_{ij} \\ B_{iij} &\mapsto B_{iij} + \frac{1}{2}r_{ij} \end{aligned} \quad (30)$$

The contribution of arc $(j \rightarrow i)$ to the system described by equation (30) can be taken to represent a



with mass-action kinetics (offset by a reaction $sp_i \rightarrow [1 - \text{sign}(r_{ij})] sp_i$ with equal magnitude rate constant), where x_i measures the standardized deviation of the population of species i from its steady state value.

After all arcs in E_G have been accounted for, the system S is stabilized by adding a multiple of the identity matrix to A so as to bring $\text{Re}(\lambda_{\text{ls}})$ to -1, as described in section 6 above (thereby including all one-loops $(i \rightarrow i)$ in the final structure G).

We then investigate the effects of perturbations $\delta \mathbf{c}$ and $\Delta \mathbf{c}$, as defined by equation (8), on the determinant $\pm F_n$ and eigenvalue stability $\text{Re}(\lambda_{\text{ls}})$. Taking $\Delta \mathbf{c}$ to be fixed and $\delta \mathbf{c}$ to be a random vector with covariance matrix $\sigma^2 I$ (and vanishing mean), and defining for any function U of the parameters (A, B, \mathbf{c}) of the system about its steady state,

$$u_i = \frac{\partial U}{\partial c_i} \quad (32)$$

and

$$W_{ij} = \frac{\partial^2 U}{\partial c_i \partial c_j} = \frac{\partial^2 U}{\partial c_j \partial c_i} \quad (33)$$

the variances and covariances of the changes δU and $\Delta\delta U$ to the arbitrary function U resulting from the random perturbation $\delta\mathbf{c}$ in the presence of the fixed perturbation $\Delta\mathbf{c}$ may be derived from

$$\begin{aligned} \langle\langle\delta U \delta U\rangle\rangle_\delta &= \sum_{i,j} \frac{\partial U}{\partial c_i} \frac{\partial U}{\partial c_j} \langle\langle\delta c_i \delta c_j\rangle\rangle_\delta \quad (34) \\ &= \sigma^2 \mathbf{u} \cdot \mathbf{u} \\ \langle\langle\delta U \Delta\delta U\rangle\rangle_\delta &= \sigma^2 \sum_{i,j} \frac{\partial U}{\partial c_i} \frac{\partial^2 U}{\partial c_j \partial c_i} \Delta c_j \\ &= \sigma^2 \mathbf{u}^T W \Delta\mathbf{c} \\ \langle\langle\Delta\delta U \Delta\delta U\rangle\rangle_\delta &= \sigma^2 \sum_{i,j,k} \frac{\partial^2 U}{\partial c_j \partial c_i} \frac{\partial^2 U}{\partial c_k \partial c_i} \Delta c_j \Delta c_k \\ &= \sigma^2 (W \Delta\mathbf{c}) \cdot (W \Delta\mathbf{c}) \end{aligned}$$

As discussed in section 4 above, we use the correlation equation (11) as a proxy metric to investigate the propensity of a system towards signal integration. For the reasons discussed in section 6, we consider eigenvalue stability-normalized perturbations satisfying

$$\langle\langle[\delta\text{Re}(\lambda_{\text{ls}})]^2\rangle\rangle_\delta = \phi^2 \quad (35)$$

where ϕ is a constant across all systems considered. Taking $U = \text{Re}(\lambda_{\text{ls}})$ and employing equation (34), obtain

$$\langle\langle[\delta\text{Re}(\lambda_{\text{ls}})]^2\rangle\rangle_\delta = \sigma^2 \sum_i \left[\frac{\partial \text{Re}(\lambda_{\text{ls}})}{\partial c_i} \right]^2 \quad (36)$$

thus implying

$$\sigma^2 = \left(\sum_i \left[\frac{\partial \text{Re}(\lambda_{\text{ls}})}{\partial c_i} \right]^2 \right)^{-1} \phi^2 = \frac{\phi^2}{\mathbf{u}_{\text{es}} \cdot \mathbf{u}_{\text{es}}} \quad (37)$$

where \mathbf{u}_{es} is the gradient vector of the eigenvalue stability $U_{\text{es}} = \text{Re}(\lambda_{\text{ls}})$ with respect to the dynamic offset vector \mathbf{c} . Similar normalization of the interacting perturbation $\Delta\mathbf{c}$ then requires:

$$\langle\langle\Delta c_i \Delta c_j\rangle\rangle_\Delta = \frac{\Phi^2}{\mathbf{u}_{\text{es}} \cdot \mathbf{u}_{\text{es}}} \delta_{ij} \quad (38)$$

where Φ is, again, a system-independent constant, and we now consider $\Delta\mathbf{c}$ to be drawn from a probability distribution with vanishing mean $\langle\Delta\mathbf{c}\rangle = \mathbf{0}$ and covariance matrix proportional to the identity (similar to $\delta\mathbf{c}$ above). Equations (34) - (38) together with equation (11) imply

$$\text{Corr}_\delta(\delta U, \delta U + \Delta\delta U) = 1 - \Phi^2 \Upsilon_{U;\Delta} + \text{H.O.T.} \quad (39)$$

where the Δ -correlation susceptibility $\Upsilon_{U;\Delta}$ is given by

$$\Upsilon_{U;\Delta} = \frac{1}{2\Phi^2} \left[\frac{(W \Delta\mathbf{c}) \cdot (W \Delta\mathbf{c})}{\mathbf{u} \cdot \mathbf{u}} - \left(\frac{\mathbf{u} \cdot W \Delta\mathbf{c}}{\mathbf{u} \cdot \mathbf{u}} \right)^2 \right] \quad (40)$$

The quantity $\Phi^2 \Upsilon_{U;\Delta}$ represents the degree to which $\text{Corr}_\delta(\delta U, \delta U + \Delta\delta U)$ is reduced in the context of the interacting perturbation $\Delta\mathbf{c}$ normalized to produce a first-order change $\Delta\text{Re}(\lambda_{\text{ls}})$ of mean-square magnitude

$$\langle\langle[\Delta\text{Re}(\lambda_{\text{ls}})]^2\rangle\rangle_\Delta = \Phi^2 \quad (41)$$

The Δ -correlation susceptibility $\Upsilon_{U;\Delta}$ depends not only on the particular system under consideration but also on the choice of perturbation $\Delta\mathbf{c}$. As we are interested ultimately in characterizing the propensity of systems themselves toward signal integration or independence, we now further average over the interacting signal $\Delta\mathbf{c}$ to define the (average) correlation susceptibility,

$$\Upsilon_U = \langle\Upsilon_{U;\Delta}\rangle_\Delta \quad (42)$$

Υ_U (equation (42)) is henceforward referred to as simply the correlation susceptibility.

Figure 4 provides boxplots of the correlation susceptibilities Υ_U for random digraph-, scale-free-, small-world-, and lattice-structured systems (see appendix A for details regarding directed network structures) generated as described above. ANOVA models of the logged correlation susceptibilities against the six network groupings shown in figure 4 indicate significant effects (determinant $F_{5,594} = 9.68$ with $p < 10^{-8}$ and $R^2 = 0.075$, eigenvalue stability $F_{5,594} = 40.41$ with $p < 10^{-16}$ and $R^2 = 0.25$).

As expected, figure 4 shows that the random digraph systems (**rdg**, **rdg10**, and **rdg20**) have progressively lower determinant- and eigenvalue stability-correlation susceptibilities as the arc density increases. We can now also compare the more complex scale-free (**sf**) and small-world (**sw** and **latt**) structured systems, however: both of these forms of structure result in lowered correlation susceptibility (determinant and eigenvalue stability) when compared with random digraphical systems of the same arc density. In section 8, we pursue structural metrics on the basis of the arc density arguments made in section 5 designed to predict correlation susceptibility.

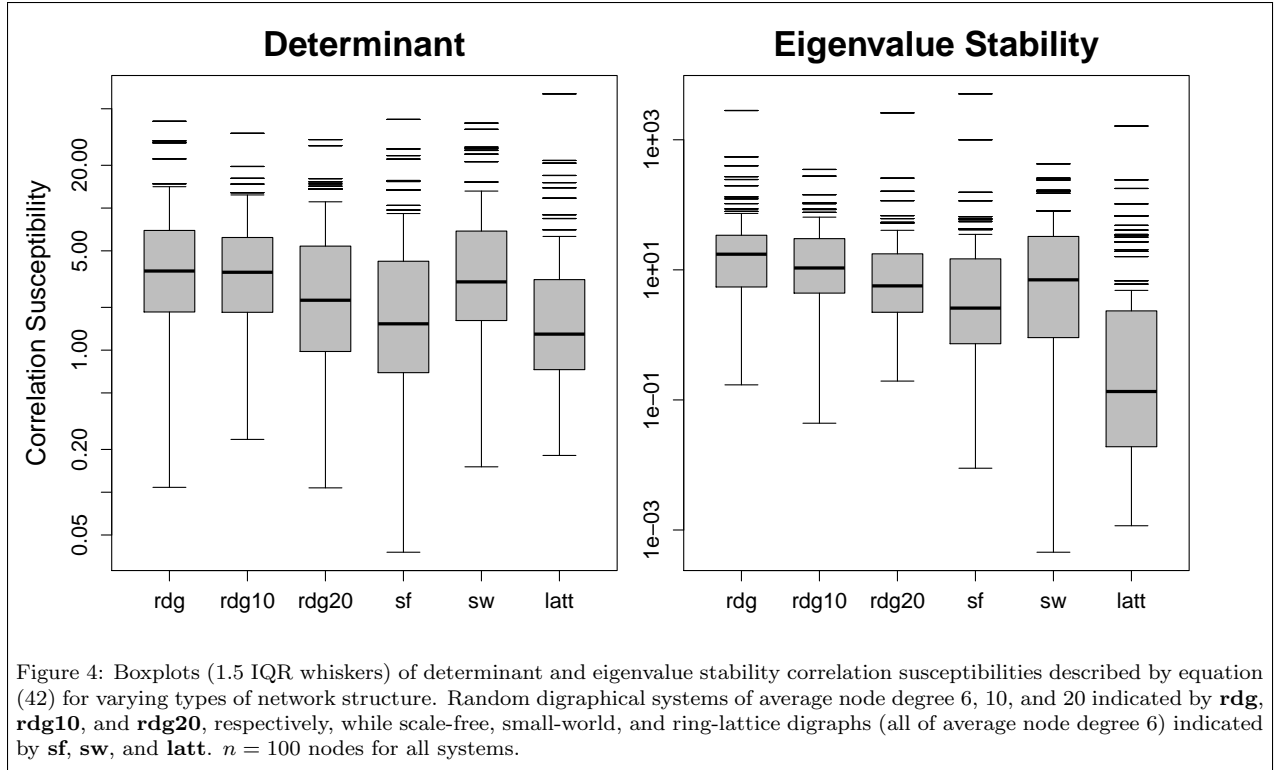


Figure 4: Boxplots (1.5 IQR whiskers) of determinant and eigenvalue stability correlation susceptibilities described by equation (42) for varying types of network structure. Random digraphical systems of average node degree 6, 10, and 20 indicated by **rdg**, **rdg10**, and **rdg20**, respectively, while scale-free, small-world, and ring-lattice digraphs (all of average node degree 6) indicated by **sf**, **sw**, and **latt**. $n = 100$ nodes for all systems.

8 Relevant Structural Metrics

In sections 5 - 7, it has been argued that increasing network arc density leads to decreased values of our proxy for signal integration, correlation susceptibility (both of the determinant and of the eigenvalue stability). One might expect, however, that not all arcs have an equal degree of influence on correlation susceptibility; both the weight A_{ji} of an arc ($i \rightarrow j$) and the location of its termini i and j in the network suggest themselves as important factors to consider. Thus we seek a scalar metric derived from the linearization matrix A in the form of a sum of normalized arc weights, with the normalization factor hopefully capturing some of the influence of arc locality.

It is not immediately obvious how to go about constructing such a normalization factor from the linearization matrix A . For the sake of clarity and parsimony, we begin by postulating that, since system stability is largely a function of the least-stable eigenvalue(s) λ_{ls} of A , the eigenvector(s) associated with λ_{ls} may offer a useful first indication to the relative influence of the various system nodes in questions of stability.

Let \mathbf{v} be (one of) the (generally complex) least-stable eigenvector(s) of the linearization matrix A ,

normalized so that $\mathbf{v} \cdot \mathbf{v} = 1$. We here define the *normalized arc density* ρ_A by

$$\rho_A = \sum_{(i \rightarrow j) \in E_G} |A_{ji}| |v_i|^2 |v_j|^2 \quad (43)$$

For systems constructed as described in section 7, there will almost always be either exactly one (if λ_{ls} is real) or two (if λ_{ls} is complex) least stable eigenvectors. When λ_{ls} is complex, the two least stable eigenvectors will be complex conjugates of each other; this implies that the value of ρ_A as defined by equation (43) will be independent of which eigenvector is chosen.

Figure 5 shows the association of the correlation susceptibility and the normalized arc density ($R^2(\log(\Upsilon_{\det}), \log(\rho_A)) = 0.10$, $R^2(\log(\Upsilon_{es}), \log(\rho_A)) = 0.35$). Considering only R^2 , the normalized arc density thus appears to explain more of the influence of network structure on correlation susceptibility than the ANOVA (section 7) on the network groupings themselves (this is not a completely fair comparison, however, since the normalized arc density includes more detailed information arising from the arc weights A_{ij}). Additionally, the normalized arc density is capable of differentiating network structures with

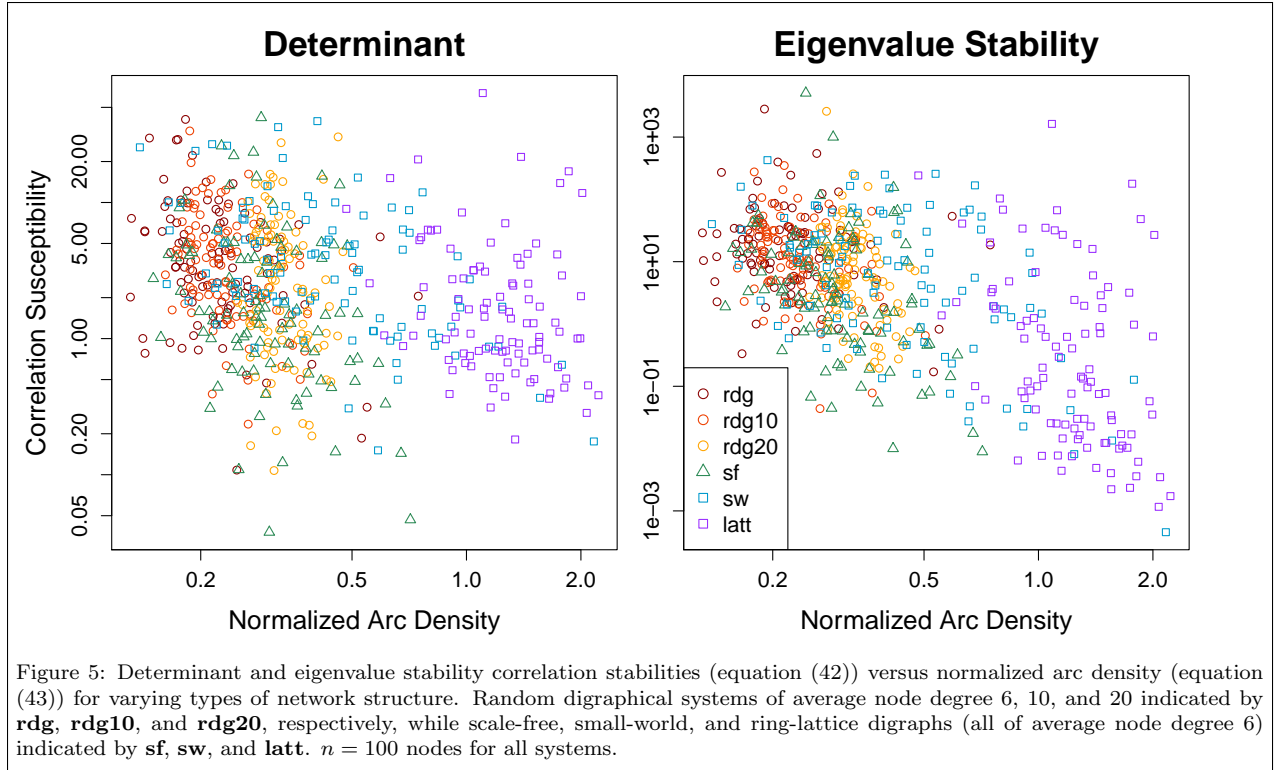


Figure 5: Determinant and eigenvalue stability correlation stabilities (equation (42)) versus normalized arc density (equation (43)) for varying types of network structure. Random digraphical systems of average node degree 6, 10, and 20 indicated by **rdg**, **rdg10**, and **rdg20**, respectively, while scale-free, small-world, and ring-lattice digraphs (all of average node degree 6) indicated by **sf**, **sw**, and **latt**. $n = 100$ nodes for all systems.

the same “raw” arc density: consulting table 1, note that scale-free and, especially, small-world networks generally have larger normalized arc densities than random digraphs of the same average degree.

Equation (43) considers only the magnitudes of the components of the least-stable eigenvector(s) \mathbf{v} . Considering equation (7), however, we see that the characteristic polynomial (and hence ultimately the eigenvalues) of the linearization matrix A depend on sums of products of the weights of arcs making up permutation k -terms. If, for example, the weights A_{12} and A_{21} change as the result of a perturbation by δA_{12} and δA_{21} , the resulting change to the weight of the

k -term $K = (1 \leftrightarrow 2)$ is

$$\delta w_K = A_{12}\delta A_{21} + \delta A_{12}A_{21} \quad (44)$$

This quantity depends on the relative phases of the arc weight perturbations, which will in turn depend on the relative phases of the perturbations to the components of the system steady state vector. Thus, we might suspect that the phases, as well as the magnitudes, of the components of the least-stable eigenvector(s), contain information relevant to the correlation susceptibility of a system.

Thus, letting $\Xi = [A^{-1}(A^{-1})^T]$, define the *eigen-*

| | Υ_{det} | Υ_{es} | ρ_A | Ψ_A |
|-------|-------------------------|------------------------|-----------------|-------------------|
| rdg | 3.6 ± 3.1 | 17 ± 19 | 0.22 ± 0.05 | 0.015 ± 0.010 |
| rdg10 | 3.5 ± 3.0 | 11 ± 13 | 0.23 ± 0.05 | 0.012 ± 0.009 |
| rdg20 | 2.2 ± 2.4 | 5.7 ± 7.6 | 0.32 ± 0.05 | 0.012 ± 0.008 |
| sf | 1.5 ± 1.7 | 2.6 ± 3.6 | 0.29 ± 0.08 | 0.018 ± 0.016 |
| sw | 3.0 ± 3.0 | 7.0 ± 10 | 0.40 ± 0.21 | 0.016 ± 0.013 |
| latt | 1.3 ± 1.1 | 0.13 ± 0.20 | 1.2 ± 0.39 | 0.030 ± 0.026 |

Table 1: Median \pm MAD values for determinant and eigenvalue stability correlation susceptibilities (equation (42)), normalized arc densities (equation (43)), and eigenvector contractions (equation (45)) for the systems used to generate figures 4 - 5.

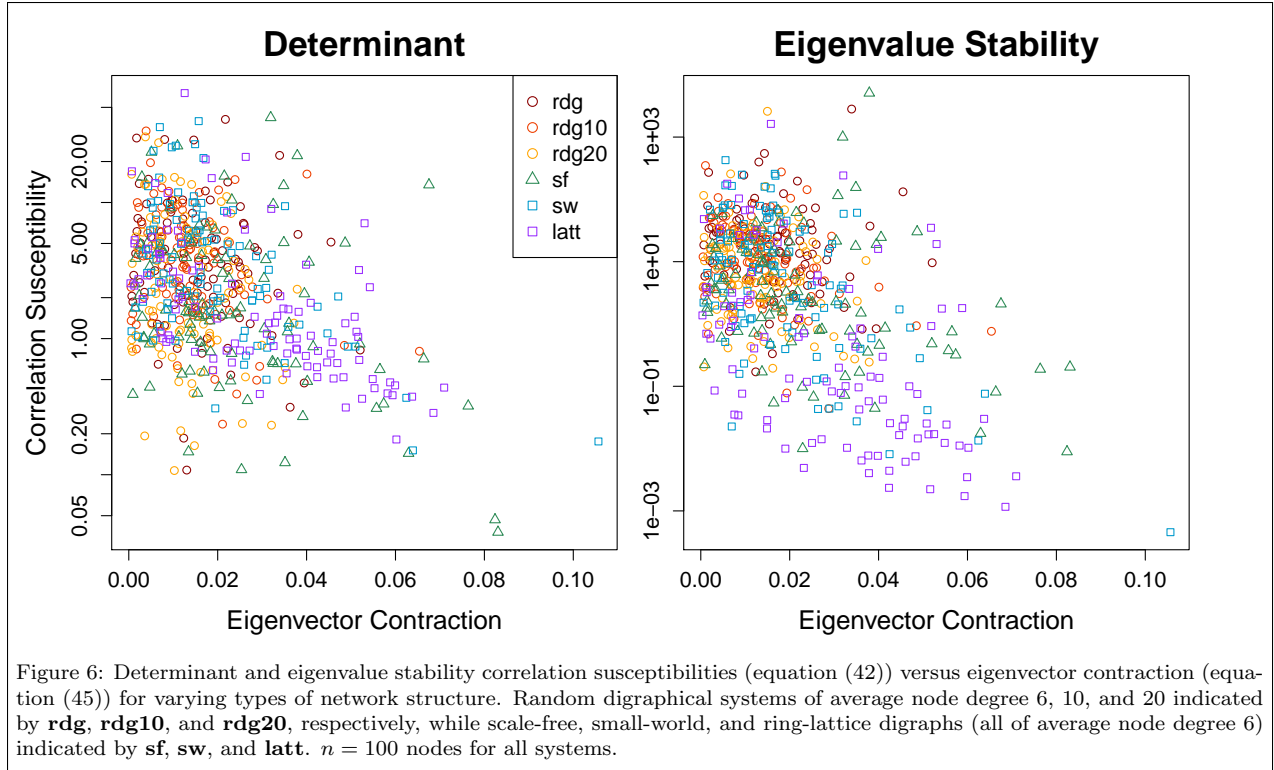


Figure 6: Determinant and eigenvalue stability correlation susceptibilities (equation (42)) versus eigenvector contraction (equation (45)) for varying types of network structure. Random digraphical systems of average node degree 6, 10, and 20 indicated by **rdg**, **rdg10**, and **rdg20**, respectively, while scale-free, small-world, and ring-lattice digraphs (all of average node degree 6) indicated by **sf**, **sw**, and **latt**. $n = 100$ nodes for all systems.

vector contraction by

$$\Psi_A = \left| \frac{\sum_i \Xi_{ii} v_i}{\text{Tr}(\Xi)} \right| \quad (45)$$

(Equation (45) is again generally independent of the choice of least-stable eigenvector when λ_{ls} is complex, since the absolute value is invariant with respect to complex conjugation of its argument.) Note that Ψ_A is a weighted sum of the (phased) components of the least stable eigenvector \mathbf{v} , with the weightings provided by the diagonal elements of the matrix Ξ . This choice of weighting was motivated by the observation that

$$\langle \langle \delta y_i \delta y_j \rangle \rangle_{\delta} = \sigma^2 \sum_k A_{ik}^{-1} A_{jk}^{-1} = \sigma^2 \Xi_{ij} \quad (46)$$

(derived from $\text{Cov}(\delta \mathbf{c}) = \sigma^2 \mathbf{I}$ and equation (9)). That is, we weight more heavily those components of the least stable eigenvector corresponding to nodes whose components in the steady state vector \mathbf{y} undergo larger variance under the perturbations $\delta \mathbf{c}$.

Figure 6 plots the correlation susceptibility against the eigenvector contraction metric ($R^2(\log(\Upsilon_{\text{det}}), \Psi_A) = 0.19$, $R^2(\log(\Upsilon_{\text{es}}), \Psi_A) =$

0.27). Once again, the R^2 values of this metric are larger than those of the ANOVA from section 7 on the network groupings — especially, in this case, with regard to the determinant correlation susceptibility. Compared to the normalized arc density, however, the eigenvector contraction has a relatively large within-network-group MAD-to-median ratio, indicating that this factor perhaps helps to explain more of the within-group variance in correlation susceptibility.

The correlation of the eigenvector contraction and the two correlation susceptibilities is negative, similar to the relationship between normalized arc density and correlation susceptibilities. Following the arguments made in section 5, one might consider the relative impact of in-phase- versus out-of-phase-perturbations to the arc weights (originating from perturbations $\delta \mathbf{y}$ to the system steady state) on the first- as compared to the second-derivatives of the k -terms composing the characteristic polynomial F_k . For the sake of brevity, this paper does not continue on this path, noting only the empirical correlation between contraction and susceptibility.

Table 2 provides the results of regression fits

$$\log(\widetilde{\Upsilon}_U) = \beta_{\log(\rho_A)}^U \log(\widetilde{\rho}_A) + \beta_{\Psi_A}^U \widetilde{\Psi}_A \quad (47)$$

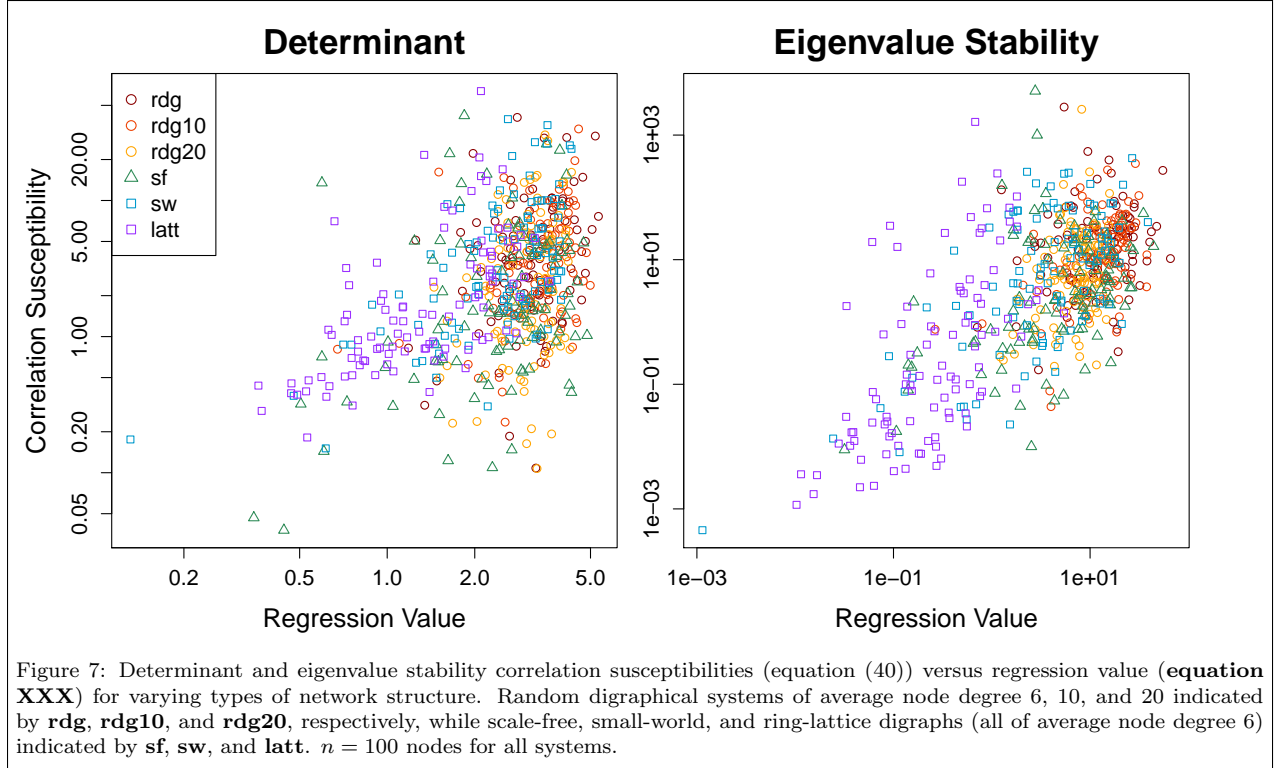


Figure 7: Determinant and eigenvalue stability correlation susceptibilities (equation (40)) versus regression value (equation XXX) for varying types of network structure. Random digraphical systems of average node degree 6, 10, and 20 indicated by **rdg**, **rdg10**, and **rdg20**, respectively, while scale-free, small-world, and ring-lattice digraphs (all of average node degree 6) indicated by **sf**, **sw**, and **latt**. $n = 100$ nodes for all systems.

| | Estimate | Std Error | Pr(> t) |
|------------------------------------|----------|-----------|-----------|
| $\beta_{\log(\rho_A)}^{\det}$ | -0.171 | 0.040 | 1.87E-5 |
| $\beta_{\Psi_A}^{\det}$ | -0.363 | 0.040 | 6.66E-19 |
| $\beta_{\log(\rho_A)}^{\text{es}}$ | -0.459 | 0.033 | 3.53E-38 |
| $\beta_{\Psi_A}^{\text{es}}$ | -0.339 | 0.033 | 7.67E-23 |

Table 2: Standardized regression coefficients for models described by equation (47). The resulting fits have $R_{\det}^2 = 0.21$ and $R_{\text{es}}^2 = 0.45$.

for U either determinant or eigenvalue stability; here we use the tilde notation $\tilde{X} = \frac{X - \hat{\mu}_X}{\hat{\sigma}_X}$ for a random variable X with estimated mean $\hat{\mu}_X$ and estimated standard deviation $\hat{\sigma}_X$. Figure 7 plots (on the original scale) the true correlation susceptibility values against their regression values.

9 Conclusions

This paper considers the behavior of the correlation of two quantities, the determinant $\det(A)$ and the eigenvalue stability $\text{Re}(\lambda_{\text{ls}})$, associated with the system linearization A under the influence of perturbations of the system dynamics of the form equation

(8). These correlations are presented as indicators of the degree to which distinct signal inputs interact cooperatively versus acting independently. The necessity of normalization of the perturbation magnitudes leads to the introduction of the correlation susceptibility (equations (39) - (42)).

Sections 5 - 6 suggest that increasing network arc density may decrease the determinant and eigenvalue correlation susceptibilities. Section 7 confirms this suggestion via simulation for a class of quadratic dynamic systems, while also indicating similar trends with regard to network clustering and degree heterogeneity. Section 8 constructs a structural metric, the normalized arc density (equation (43)), which provides a potential unified explanation for the impacts of these distinct aspects of network structure.

The results with regard to (normalized) arc density are somewhat reminiscent of the dimensionality dependence of mean field theory in statistical physics [7]. An Ising model spin is less sensitive to fluctuations of a nearby spin in a higher dimensional/higher connectivity lattice in a manner similar to the decreasing sensitivity of the response to one perturbation with respect to the influence of another in the dynamic systems studied here as normalized arc density increases.

Section 8 also introduces the eigenvalue contraction metric, which appears to offer a predictor of the correlation susceptibilities complementary to the normalized arc density. Both the network density and the eigenvalue contraction focus on the nodes most involved in the least stable eigenvector(s) of the linearization A , which may be loosely thought of as the points at which the network is most susceptible to destabilization.

The results with regard to the normalized arc density and eigenvector contraction indicate that networks with lower arc density in the neighborhood of these focal nodes, and for which the fluctuations of the dynamic variables associated with these nodes are anticorrelated/out-of-phase with regard to the least stable dynamic modes, are more likely to respond to multiple signal inputs in a cooperative manner. It is intriguing to contemplate extension of this idea to develop more easily calculable (i.e., not linearization A -eigendecomposition-dependent) system structural metrics for potential use as predictors of the degree of interaction between distinct perturbations (such as, for example, an infection and a drug treatment).

Appendices

A Generation of Directed Network Structures

Random digraph structures were generated by independently adding each arc ($i \rightarrow j$) to the digraph with a fixed probability $p_{\text{arc}} = \frac{d}{n-1}$, where the parameter d controls the average node in- and out-degree and n is the number of nodes in the network.

Directed scale-free networks with n nodes and $2nd$ arcs were generated in a manner similar to the Barabasi preferential attachment mechanism [8]. First, $(d+1)$ fully connected nodes were added. Then $n - (d+1)$ nodes were added sequentially one-by-one, with d arcs added directed from the newly added node to old nodes and d arcs added from old nodes to the new node at each step. For each of these $2d$ new arcs, the identity of the adjacent old node (whether it be tail or head of the new arc) was chosen at random with non-uniform probability proportional to the sum of the in- and out-degrees of the old node (subject to the constraint that no two arcs may connect the same pair of nodes with the same directionality).

Small-world digraphs with n nodes and $2nd$ arcs

(where d is even) were generated starting with a ring lattice in which each node is connected bidirectionally to the $\frac{d}{2}$ nearest nodes in each direction, then rewiring each directed arc with probability p_{rw} . Similar to the mechanism described by Watts, et. al. [9], each rewired arc has one terminus (head or tail chosen randomly with uniform probability) changed to a node chosen randomly from all nodes in the system with uniform probability, again constrained to prevent any two arcs from sharing both the same tail and the same head.

References

- [1] D.B. Doroquez and I. Rebay. Signal integration during development: mechanisms of EGFR and Notch pathway function and cross-talk. *Critical reviews in biochemistry and molecular biology*, 41(6):339–385, 2006.
- [2] J. Silva and A. Smith. Capturing pluripotency. *Cell*, 132(4):532–536, 2008.
- [3] D.C. Wylie. Linked by loops: Network structure and switch integration in complex dynamical systems. *Physica A: Statistical Mechanics and its Applications*, 388(9):1946–1958, 2009.
- [4] H. Schneider and G.P. Barker. *Matrices and linear algebra*. Dover Publications, 1989.
- [5] C.J. Puccia and R. Levins. *Qualitative modeling of complex systems*. Harvard Univ. Pr., 1985.
- [6] J. Landin. *An introduction to algebraic structures*. Dover Publications, 1989.
- [7] N. Goldenfeld. *Lectures on phase transitions and the renormalization group*. Addison-Wesley, Advanced Book Program, Reading, 1992.
- [8] A.L. Barabási and R. Albert. Emergence of scaling in random networks. *Science*, 286(5439):509, 1999.
- [9] D.J. Watts and S.H. Strogatz. Collective dynamics of ‘small-world’ networks. *Nature*, 393(6684):440–442, 1998.